Efficiency and profitability of second life automotive batteries for renewable sources power plants

Journal of Energy Storage 145 (2026) 119897

Contents lists available at ScienceDirect

Journal of Energy Storage

journal homepage: www.elsevier.com/locate/est

Research Papers

Efficiency and profitability of second life automotive batteries for renewable sources power plants

Alberto Ponso [a],*, Eleonora Cerva [b], Nicholas Monticone [b], Rocco Sorace [b], Angelo Bonfitto [a], Andrea Tonoli [a]

[a] Politecnico di Torino. Center for Automotive Research and Sustainable Mobility (CARS). Dipartimento di Ingegneria Meccanica e Aerospaziale (DIMEAS), Corso Duca degli Abruzzi 24, Turin, 10129, TO, Italy

[b] CVA – Compagnia Valdostana delle Acque. Divisione Efficienza energetica ed Open innovation, Via Stazione 31, Châtillon, 11024, AO, Italy

ARTICLE INFO

Keywords:
Stationary battery storage systems
Second life batteries
Non-programmable renewable energy sources
Circular economy

ABSTRACT

Mobility electrification is considered among the main pillars for decarbonization of modern society, a crucial challenge in light of the ever growing impacts of human activities on Earth's climate. The cost of batteries is a significant factor slowing down the diffusion of electric vehicles (EVs) and their disposal still presents open criticalities. On the other hand, to achieve larger shares of renewable electricity generation, installation of battery accumulators is needed to support production from non-programmable sources, such as free-flow hydroelectric plants or photovoltaic parks. Their realization with recycled modules coming from automotive application helps addressing the two issues altogether and represents a cheaper alternative to first life batteries. This article presents the experimental results of the installation of a large-scale storage system to improve the profitability of a free-flow hydraulic plant. The main novelty coming from the project is the application of a mix of second life and new modules, to compare their performance in the same operating environment. On-field behavior of the two subsystems has been used to analyze the respective profitability, in light of historic price trends and real production program of the free-flow hydraulic plant. The results show a faster return of investment for the second life subsystem.

1. Introduction

The last centuries have seen a significant uptrend of temperatures compared to the previous period, as highlighted by the current increase of over 1.0 °C above pre-industrial levels [1]. Since 1975, the rate of global warming has accelerated, with a pace of +0.2 °C per decade [2], a trend that has its main causes in greenhouse gases (GHG) coming from human activities [3]. Transportation is one of the economic sectors most responsible for carbon emissions, as it produced 7.6 billions of tonnes of carbon dioxide in 2020, around 20% of human-caused CO_2 [4]. Given this role as polluter and the maturity of electrification solutions, it is evident that sustainable mobility has a great potential in decarbonization efforts [5].

Electric transit has been a reality for more than a century, as its first application to a passenger railway dates back to 1881 [6]. However, its mass deployment in private vehicles came only as a consequence of the commercial introduction of lithium-ion batteries (LIBs) [7]. Moreover, to present day, technical limitations still affect electric vehicles (EVs) in their design phase, such as the low energy density of LIBs, in the order of hundreds of Wh/kg [8,9]. This is particularly relevant in the comparison between traditional vehicles and EVs, as it requires to strike a balance between a capacity large enough for a satisfactory range and a small weight increase compared to the petrol-powered equivalent. In addition to this, batteries experience degradation throughout their life, with a reduction in capacity that occurs from usage and time flow [10]. The result is a decrease of the traveling range from the first day of life of the car, a phenomenon which further worsens the technical issues affecting EVs [11]. For this reason, traction batteries have a limited operational life, which ends when the available capacity drops below 70%–80% of the nominal one [12,13]. Battery degradation exponentially accelerates after it reaches a point, called knee, which generally takes place when capacity degraded to levels between 70 and 80% of the nominal value. The onset of this phenomenon can be moved forward by reducing cell charge voltage [14]. Furthermore, it was found that coating the NCM cathode with Al_2O_3 [15] and introducing chemical additives in the electrolyte can further delay the emergence of these knees [16]. During batteries' first life, preventing

* Corresponding author.
E-mail address: alberto.ponso@polito.it (A. Ponso).

https://doi.org/10.1016/j.est.2025.119897
Received 5 December 2024; Received in revised form 4 October 2025; Accepted 12 December 2025
Available online 18 December 2025

the insurgence of this phenomenon is crucial to ensure a satisfying remaining capacity for their second life, where they are re-used in stationary applications [17].

As a consequence, a wide literature exists on the topic of knee detection and prediction. Given the difficulty of on-the-fly replacement, detection of early warning signals for scheduled battery substitution is fundamental. As an example, machine learning techniques have been employed to classify cells as ‘‘short-life’’, ‘‘medium-life’’, or ‘‘long-life’’ with as little as three charge–discharge cycles [18]. The same work also found out that the onset of the knee and the acceleration of degradation are separated by around 100 cycles, leaving time to schedule battery substitution. Analysis of the curvature in the capacity fade graphs has shown the potential for a faster knee onset detection, up to 300 cycles in advance [19]. Another technique to detect knee onset, given its correlation with anode Li plating, is differential voltage analysis, which can be conducted directly on voltage trend observed during system operation [20]. Additionally, usage of a Long-Short Term Memory (LSTM) network managed to not only predict the number of cycles until the appearance of the knee, but also the residual capacity at that point, which is important for addressing batteries towards their second life [21]. Despite its importance as a factor to identify knee onset, it is difficult to estimate battery capacity if its usage is not limited to charge and discharge cycles, but follows irregular trends, as is the case for automotive systems. Therefore, great importance is given to battery models which can predict the degradation process based on current and voltage profiles [22]. To exploit higher computational power and reduce the complexity of algorithms deployed on vehicle ECU, a solution is to implement cloud battery management system with a digital twin which logs current drawn from the battery and uses it to simulate degradation in real time [23,24].

The exponential growth in EV sales has increased LIBs demand by carmakers, which have rapidly become the main purchasers in a sector previously dominated by another large and fast-growing market such as consumer electronics [25]. Automotive industry is now the main driver of lithium and cobalt consumption, taking up respectively 60% and 30% of their global production in 2022 [26]. Raw materials employed in cells, such as lithium, cobalt and nickel, represent a significant cost and most of them are among the critical materials indicated by the European Union because of their scarcity or high supply risks [27]. Further exacerbating the issues with resources procurement for automotive industry, a third LIB application field is seeing a significant growth as well, in the form of stationary applications for battery energy storage systems (BESS) [28,29].

The increase in total installed stationary capacity is a positive factor in the path to decarbonization, as it helps utilizing renewable energy sources in a more efficient way. For example, stationary batteries can be used to store excess production from non-programmable renewable energy sources (NP-RES) such as photovoltaic (PV) plants during hours with most sunshine, to be eventually released when their production is lower [30]. Moreover, intermittent energy sources such as solar electric generators can overload the distribution grid during their peak production hours, as their output is excessive. This mismatch between demand and production leads to curtailment, i.e. reduction of power output or disconnection of electric generators from the grid. The share of energy lost because of this practice has been estimated to be above 1% in the areas with the most PV power installed in 2018 [31]. This amounts to a total of 6.5 TWh/year, enough to power a country such as Luxembourg [32]. With the constant acceleration in the installation of renewable electricity generation, the amount of lost energy increased as well, with a total of 1.3 TWh of solar and wind energy curtailed in California alone between March and April 2023 [33].

In addition to an increase of energy lost due to curtailment, the installation of more power plants based on NP-RES has the effect of reducing the profitability of the already existing plants. This phenomenon, known as price cannibalization [34], is particularly significant for photovoltaic plants, which concentrate their production in few hours, but is affecting all electricity generated from non-programmable sources, including wind farms and free-flow hydroelectric plants [35]. However, production peaks from local wind conditions can be evened out by grid interconnection, while solar production is more difficult to mitigate with grid interconnection [36]. This means that price depression is noticeable especially in the afternoon, as it is mostly driven by solar output. On the other hand, electricity demand is constantly increasing worldwide, with over 3% yearly growth, driven by data centers and household consumption [37]. While this trend keeps average electricity prices stable – despite the cannibalization due to renewable sources – the increase in EV adoption is driving them up during the hours of highest demand, i.e. early morning and late afternoon [38]. It can therefore be said that the evolution of electricity prices in the near future will see an increase in daily spread between minimum and maximum, which can be exploited to profit from daily energy trading [39]. As a consequence, BESS profitability is bound to increase in the following years thanks to electricity market evolution [40]. Therefore, BESS installation will become fundamental to ensure economic sustainability of renewable electricity generation, allowing to match demand and offer. It is therefore evident how stationary accumulators play a crucial role in the fight against global warming through increase of efficiency for electricity generation, not only from PV, but from all NP-RES such as wind farms and free-flow hydraulic plants [41].

However, similarly to what happens with automotive electrification, high cost of batteries represents an obstacle to the installation of these accumulators to support power plants, as lithium demand exceeds production volumes [26]. Despite the common issues in procurement, automotive and stationary application sectors have different use profiles and performances required to LIBs. Specific energy, measured in Wh/kg, is crucial in the design procedure of batteries for automotive applications. This is true not only in sports and racing cars, which need light and dense batteries for high performance, but also in low segment passenger cars, where weight minimization is needed to reduce energy consumption and extend driving range [42,43]. By contrast, total mass is not as relevant for stationary applications, as highlighted by the higher share of heavier lithium-iron-phosphate (LFP) batteries compared to EV market [44,45]. In addition to high purchase cost and procurement issues, LIBs present challenges at the end of their lives too, because of their severe fire hazard with consequent release of toxic substances and of the water and ground pollution coming from their improper disposal [46,47].

Recycling cells to extract raw active materials for re-use in new batteries is a solution that solves the issue of landfilling while creating value from waste. Such activity still has non-negligible economic drawbacks: price of material transportation from scrapyards to recycling plants is in the region of 500–5000 $/kg [48], while recycling procedure costs are not uniform globally, ranging between 7.5 and 50 $ per hour [49]. Moreover, although recycling avoids dispersion in the environment of precious active materials, it is less efficient than re-using, since traction batteries are still usable after their first life. Therefore it is possible that, instead of acting as competitors, carmakers and electricity producers collaborate to reciprocally solve issues, improving profitability and sustainability [50]. Usage of exhausted traction batteries to assemble stationary accumulators which support electricity generation from NP-RES is a possible way to reduce costs, as second life batteries cost between 20 and 80% of first life equivalents [51]. Moreover, it would also mitigate the higher purchase cost compared to traditional vehicles, since the market for second life batteries would ensure that older EVs still hold good monetary value [52,53]. As a matter of fact, studies conducted on Japan's market, which was among the early adopters in terms of powertrain electrification, demonstrated that repurposing of exhausted EV batteries for static installations is financially sustainable without government subsidies [54]. Integration of exhausted batteries from Nissan commercial vehicles with rooftop solar panels was already realized in 2018 in Isahaya, Japan [55,56]. Installation of BESS built from second life batteries is so competitive that it has also been shown to outperform carbon taxes as a tool to incentivate CO_2 reduction [57]. In addition to economic benefits, reusage of batteries scrapped from EVs has the potential to improve the sustainability of both electric mobility and stationary accumulators. A life cycle assessment demonstrated that battery repurpose reduces the impact on climate change by 16% compared to a new installation, for an electricity production mix below 113 gCO_2eq/kWh [58]. Therefore, their application to renewable energy sources has indeed a positive impact on the whole life cycle. The spectrum of energies employed for electric mobility ranges between some hundreds of Wh for micro-hybrid solutions and electric scooters to hundreds of kWh for the case of battery electric buses, making second life batteries attractive for different usage scenarios [59]. Particularly interesting is the match between the average size of EV batteries (40–50 kWh) and that of systems installed in residential complexes [60,61]. Application of stationary accumulators provides advantages especially to increase profitability of solar production, whose economic sustainability compared to fossil fuels is still not evident [62]. For the same reason, application of stationary accumulators is appealing to energy community projects, where over 90% of economic benefits are coming from incentives [63].

Stationary re-usage of batteries from automotive application, giving them a second life, is a well-studied topic in literature. As an example, analyses have been conducted on the realization of off-grid PV arrays which store electricity in second life batteries to then conduct EV recharge [64,65]. A similar application is being pursued by China Tower, which is progressively replacing lead–acid batteries with second life EV modules in its telecommunication towers that are not connected to electrical distribution [66]. Integration of modules retired from automotive usage to maximize PV exploitation at centralized charging stations for battery swap has also been proposed [67]. Furthermore, usage of exhausted traction batteries to perform grid support during peak demands has been investigated [68]. This cost-effective application is useful to delay expensive upgrade to distribution grids when demand is excessive only in parts of the day, as is the case with PV generation. Economic viability of second life automotive LIBs application as a mean to cut electricity purchasing cost has been studied [69]. In such context, using currents up to C/8, it was concluded that the most effective strategy is energy arbitration instead of peak shaving. This is performed by storing electricity when the cost is lower to then use it during hours with higher demand. However, savings correlated to cheaper energy purchase are low and the pay-back time exceeds ten years in this study. Application of second life batteries to local energy communities, instead, showed a payback time of 5 years for the installation of an EV battery pack (61 kWh) to maximize PV exploitation [61]. Profitability difference between these two solutions highlights the higher suitability of stationary installations at production sites rather than at consumption points, as they allow to deliver more energy, avoiding curtailment of solar panels. Analogous conclusions have been drawn for the application of second life batteries in private homes and microgrids, where BESS profitability is dependent on the presence of an already installed renewable energy source [70]. Installation of battery storage to increase profitability of power plants based on NP-RES is a well-known topic in literature, especially concerning PV plants [71–73]. Research interest on this topic is bound to increase, especially as second life batteries from automotive usage are expected to enter the market in mass, with a total capacity in the order of GWh/year by 2030 [74]. The impact of this influx of exhausted batteries on the energy market is already becoming evident, with two large-scale projects launched in the United States between late 2024 and early 2025. In November 2024, battery assembler Element Energy announced the full activation in Texas of a BESS assembled from the batteries of over 900 vehicles, with a total capacity of 53 MWh [75]. An even larger project was announced in June 2025 by battery recycler Redwood Company, which unveiled a 12 MW/63 MWh BESS assembled from second life EV batteries in support of a data center of Abilene, Texas [76]. However, none of these two systems are designed as an integration to an already existing power plant exploiting NP-RES.

The present article aims to cover the existing research gap by evaluating the additional revenue generated by installation of a stationary battery in support of electricity production plants based on NP-RES. Monetary earnings are derived from real historical trends of local electricity prices, while production programs are scaled from real examples. The study compares the impact of energy arbitration on the profitability of two non-programmable power stations, namely a free-flow hydroelectric power plant and a photovoltaic park. These economic considerations are drawn comparing the experimentally obtained efficiencies of a system assembled from recycled automotive battery modules and of a first life accumulator. On-field tests have been conducted on a BESS installed in support of a hydroelectric power plant, but their findings can be extended to the case of the photovoltaic park. As a matter of fact, experiments not only validate the battery system, but also its interaction with a generic power plant, as their connection is conducted at distribution level.

The rest of the article is structured as follows: Section 2 describes the methodology followed in the work; Section 3 describes the case study of BESS-2L project and the context of application, introducing a PV power plant as well; Section 4 presents and analyzes the experimental results and their utilization for economic assessments of storage application to a hydroelectric and a photovoltaic plant; Section 5 closes the paper by drawing conclusions based on the findings of previous Sections.

2. Methodology

This Section describes the procedure followed to evaluate the financial impact of storage integration with a power plant based on NP-RES. Although the results presented come from the operation of the system realized during the BESS-2L project, the methodology is independent from the size, geographical location and power source of the plant and can be replicated on a different scale. Moreover, the chemistry employed in the batteries has negligible influence, as operating constraints ensure that charge and discharge are always operated below unitary C-rate. These conditions, in particular, eliminate the advantage of long cyclability at high C-rates offered by the olivine structure of LFP cathodes [77]. The procedure to assess the impact of battery installation can be divided into five sequential phases, as shown in Fig. 1.

2.1. System sizing

The first step in the assessment of the battery system impact is the definition of the installed capacity. It is fundamental not only to evaluate the total investment, but it also defines the operation of the system. To conduct a complete assessment of system profitability and to identify the influence of all the factors in play, it is necessary to define a range of capacities upon which to conduct the study. To this end, power plant operating constraints need to be taken into account.

The main factor to consider is the performance of the existing power plant, which is fundamental in the identification of the capacity to install, as storage capability needs to match up with electricity production volumes. However, power output is not the only limiting factor to account for when sizing the battery. Peak operational power admitted by the transformers represents a further constraint on battery operation to be considered during scheduling.

2.2. Operation definition

2.2.1. Energy market working principle

In the evaluation of monetary impacts, it is necessary to reproduce the daily operation of the system. This requires the definition of an algorithm that schedules charge and discharge phases with the goal of maximizing revenue. The operating scheme for electricity producing plants is day-ahead planning, in which power output programming

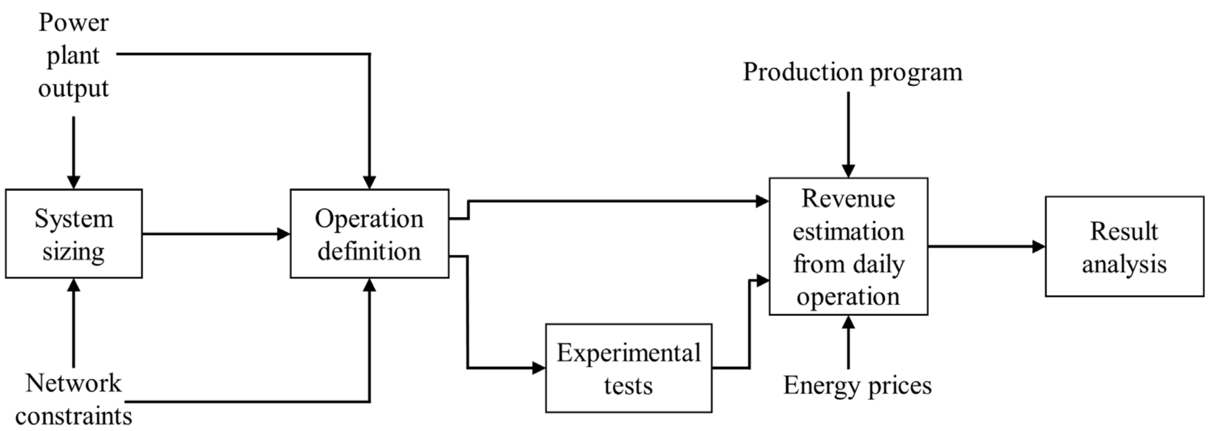

Fig. 1. Procedure for the evaluation of battery storage system impact on power plant profitability.

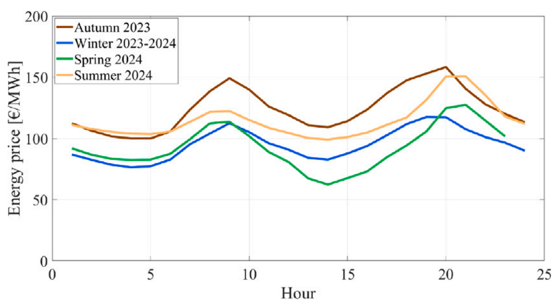

Fig. 2. Hourly energy prices in the period from September 23rd, 2023 to September 22nd, 2024.

is conducted the day before, without knowing the price that will be paid [78]. Negotiation is performed on the basis of hourly timeslots, with each one seeing a different reward for electricity producers on the basis of volumes traded in day-ahead market. Because the amount of energy exchanged on the market is orders of magnitude larger than that stored in the battery, it is safe to consider hourly prices as an independent variable for the scheduling problem. However, prices can be forecast as their profile for each day is influenced by the period of the year, the day of the week and by the presence of holidays. A prospect of price trends divided by season is shown in Fig. 2.

From the historical pattern of prices, it is possible to notice two significant peaks and two minima everyday. Night prices are lower throughout the entire year because of the low demand, while the price drop in the afternoon is less noticeable in winter, due to the lower output of solar production during daylight hours. The goal of energy storage installation is to provide the highest possible revenue for the power plant, therefore the typical operation involves two charge–discharge cycles during the day. To maximize profits, operation at low C-rates is therefore unsuitable, as it would fail to exploit price unbalances. On the other hand, energy market performs trades in timeslots of one hour, thus imposing to operate batteries at C-rates below 1.

Operation of the accumulation system via full discharge twice a day has been demonstrated as feasible for plants where only air cooling is provided, as a consequence of around 4 h of rest required after charge and discharge [79]. The equally spaced distribution of peaks and valleys in hourly prices therefore demonstrates that cycling twice a day at 1C is a feasible operating technique.

2.2.2. Input data

Daily programming of battery operation requires constantly updated data to appropriately schedule charge and discharge to maximize revenues. The first information needed is the forecast for the following day of power plant hourly output $P_{plant,i}$. Knowledge of production program, together with the transformer limit P_{max}, identifies the space of possible operation for the optimization algorithm. To maximize the revenue, hourly electricity price r_i has to be forecast in the loop of battery usage scheduling. To this goal, market results are fed to the system as soon as they are communicated by the authority regulating the exchange, generating a price database that is updated daily. Trading outcomes are also used to immediately assess monetary results from the battery usage schedule. If bad price forecasting led to unsatisfactory revenues, optimization is performed again on the basis of the exact prices resulting from day-ahead market and the arbitration is conducted a second time, on the Mercato Infragiornaliero 1 (MI1) [80].

In addition to information flows coming from outside, the scheduling algorithm requires constant feedback from storage itself. Available battery capacity C_{batt} is needed to assess the maximum energy that can be stored and is constantly monitored by the battery management system (BMS) during the life of the plant. However, the dynamic of its evolution is considerably slower than that of battery charge and discharge, with losses below 3% per year [81]. Therefore, this parameter is considered a constant in the optimization problem defining battery usage scheduling.

To evaluate the revenue from battery operation, C_{batt} alone is not sufficient. Profit provided by arbitration comes from injecting electricity to the grid when power demand is larger than when the energy is produced. However, energy conversion for storage in batteries causes a loss that affects system profitability. For the control logics aimed at maximizing the revenue, this information is represented by round-trip efficiency (RTE), defined as

$$\eta_{RTE} = \frac{E_{discharge}}{E_{charge}} \tag{1}$$

It represents the ratio between the energy absorbed from the grid during a full charge process E_{charge} and the one that the battery releases during a full discharge $E_{discharge}$. Such value has key importance in assessing economic impacts of accumulators installation to the power plant and it influences the operating program to be communicated to the energy exchange for negotiation. During the first steps of system sizing, when no experimental result is available, values of η_{RTE} are to be taken from literature, where results around 90% can be found for 1C operation [82]. After experimental tests are conducted on the installation, real value of η_{RTE} is fed to the programming algorithm and its evolution is then tracked and updated during continuous operation of the plant.

2.2.3. Optimization problem

In the following, the operation scheduling algorithm employed for the impact assessment presented in this article is described. While the economical results come from the simulation of plant operation, the algorithm itself has been installed on the real energy storage system and its communication with the BMS has been validated. Therefore, the values of C_{batt} and η_{RTE} presented in the equations defining the optimization problem are constantly updated via real time monitoring of the system. In addition to this, communication with the energy market has been implemented, so that prediction of hourly prices r_i is always conducted based on the most recent data.

The goal of the algorithm, stated in Eq. (2), is to maximize the revenue R_{tot} obtained by the power plant charging the batteries when electricity price is low and discharging them when price is high, satisfying the constraints of Eqs. (3)–(16).

$$\max_{\mathbf{P_{ch}},\mathbf{P_{dch}}} R_{tot} = \sum_{i=1}^{N_{hours}} P_{tot,i} \cdot r_i \tag{2}$$

$$P_{tot,i} = P_{plant,i} - P_{ch,i} + P_{dch,i}, \quad \forall i \in \{1, 2 \dots N_{hours}\} \tag{3}$$

$$P_{tot,i} \geq 0, \quad \forall i \in \{1, 2 \dots N_{hours}\} \tag{4}$$

$$P_{tot,i} \leq P_{max}, \quad \forall i \in \{1, 2 \dots N_{hours}\} \tag{5}$$

$$P_{ch,i} \leq \frac{C_{batt}}{1h} \cdot \frac{1}{\sqrt{\eta_{RTE}}}, \quad \forall i \in \{1, 2 \dots N_{hours}\} \tag{6}$$

$$P_{dch,i} \leq \frac{C_{batt}}{1h} \cdot \sqrt{\eta_{RTE}}, \quad \forall i \in \{1, 2 \dots N_{hours}\} \tag{7}$$

$$P_{ch,i} \leq P_{max,inv} \cdot \frac{1}{\sqrt{\eta_{RTE}}}, \quad \forall i \in \{1, 2 \dots N_{hours}\} \tag{8}$$

$$P_{dch,i} \leq P_{max,inv} \cdot \sqrt{\eta_{RTE}}, \quad \forall i \in \{1, 2 \dots N_{hours}\} \tag{9}$$

$$P_{dch,i} \cdot P_{ch,i} = 0, \quad \forall i \in \{1, 2 \dots N_{hours}\} \tag{10}$$

$$\sum_{i=1}^{N_{hours}} P_{ch,i} \cdot \sqrt{\eta_{RTE}} \leq \frac{2C_{batt}}{1h} \tag{11}$$

$$\sum_{i=1}^{N_{hours}} P_{dch,i} \cdot \frac{1}{\sqrt{\eta_{RTE}}} \leq \frac{2C_{batt}}{1h} \tag{12}$$

$$\sum_{i=1}^{j} P_{ch,i} \cdot \sqrt{\eta_{RTE}} - P_{dch,i} \cdot \frac{1}{\sqrt{\eta_{RTE}}} \geq 0, \quad \forall j \in \{1, 2 \dots N_{hours}\} \tag{13}$$

$$\sum_{i=1}^{j} P_{ch,i} \cdot \sqrt{\eta_{RTE}} - P_{dch,i} \cdot \frac{1}{\sqrt{\eta_{RTE}}} \leq \frac{C_{batt}}{1h}, \quad \forall j \in \{1, 2 \dots N_{hours}\} \tag{14}$$

$$\sum_{i=1}^{N_{hours}} P_{ch,i} \cdot \sqrt{\eta_{RTE}} - P_{dch,i} \cdot \frac{1}{\sqrt{\eta_{RTE}}} = 0 \tag{15}$$

$$\sum_{i=j}^{j+3} P_{ch,i} \cdot \sqrt{\eta_{RTE}} + P_{dch,i} \cdot \frac{1}{\sqrt{\eta_{RTE}}} \leq C_{batt}, \quad \forall j \in \{1, 2 \dots N_{hours} - 3\} \tag{16}$$

Eq. (3) defines $P_{ch,i}$ and $P_{dch,i}$ as the charge and discharge power as measured at the point of delivery (POD) to the network, downstream of inverter stages, where output power is measured for revenue computation. Inequalities (4) and (5) represent lower and upper boundary on system total output, which cannot absorb energy from the grid and is constrained by transformers operating limits. Inequalities (6) and (7) translate battery operation at no more than 1C into constraints on decision variables $P_{ch,i}$ and $P_{dch,i}$ through battery round-trip efficiency η_{RTE}. Such constraints are further tightened by inequalities (8) and (9), which ensure that the inverters linking batteries to the distribution grid are not overloaded. Eq. (10) represents the impossibility to have both charge and discharge in the same timeslot. Inequalities (11) and (12) represent the constraint to limit the number of charges and discharges to two during the day. Inequality (13) ensures that the system never discharges more than what is in storage, Inequality (14) avoids overcharging, while (15) constrains the SoC at the end of the day to be the same as that at the beginning of the day. This constraint comes from the fact that intra-day oscillations are significantly larger than inter-day oscillations and therefore it is sub-optimal to keep energy stored for the following day. Finally, Inequality (16) imposes a rest of four hours between every charge and discharge phase, to allow for system cooling.

2.3. Experimental tests

Because of the critical importance of η_{RTE} to assess system profitability, on-field tests must be performed on the real system to evaluate its performances. To this purpose, charge–discharge tests are needed, so that energy absorbed and injected in the grid can be measured. Constant low current charge–discharge cycles are common in the field of battery testing as a way to experimentally determine the total capacity of the system through Coulomb counting [83,84].

However, for the purpose of these experiments, total plant capacity is not the most important parameter to assess. What is relevant to be determined for profitability evaluation is the ratio between the energy delivered and that absorbed when the batteries are operated at constant power, to replicate usage conditions during energy arbitration. Therefore, the tests are based off constant power charges and discharges at rates close to the limits allowed by the inverters $P_{max,inv}$. In this way, it is possible to determine η_{RTE} in the operating conditions.

Furthermore, by imposing powers that match those required by real operating conditions, it is also possible to validate the design of the containers hosting the batteries, monitoring cell temperatures. Since heat generation increases with the power, conduction of low current capacity tests would not provide any information about the performances of thermal management system. Emulating everyday operation, on the other hand, it is possible to obtain a realistic temperature profile, which allows to evaluate the thermal safety of the subsystem realized from second life battery modules.

2.4. Revenue estimation

After the range of capacities for the study has been identified, everyday operation of the system has been defined and η_{RTE} has been determined experimentally, energy arbitration revenues have to be found as a function of battery capacity. To this goal, it is necessary to simulate system operation and its interaction with the power plant and the energy market.

To compare the results of first and second life batteries, two plants are simulated, one supported by a fresh storage system, the other by second life modules. Electricity production is recreated from the power output of previous years. For economical evaluations, historical trends of energy cost are available from the authority managing the power exchange [85].

At the end of the simulation, for every storage capacity, the following results are obtained: (1) first life optimized revenue $R_{opt,1L}$, corresponding to the total revenue of the plant obtained with the installation of the first life batteries; (2) first life best revenue $R_{best,1L}$, corresponding to the revenue that could be obtained if prices were known in advance; (3) second life optimized revenue $R_{opt,2L}$ and (4) second life best revenue $R_{best,2L}$, the equivalent of $R_{opt,1L}$ and $R_{best,1L}$ for the plant with second life batteries. These results are to be compared with base revenue R_{base}, obtained by the plant without the installation of any energy storage system.

a)   b)

Fig. 3. Photographies of the real system installed during the project. (a) The two containers housing first life and second life batteries. (b) Interior of the second life container.

2.5. Result analysis

To properly evaluate the economic performance of the two subsystems, relevant metrics need to be defined on the basis of simulation results. First, the revenue increase is introduced, defined as

$$R_{increase} = R_{opt} - R_{base}. \tag{17}$$

The value of $R_{increase}$ needs to be normalized by the additional revenue provided by the energy storage system against the original revenue of the plant, to effectively describe energy storage effect on plant profitability. This is done as

$$R_{inc,pct} = \frac{R_{opt} - R_{base}}{R_{base}} \cdot 100, \tag{18}$$

which allows to compare the impact of batteries regardless of plant size. Moreover, the additional revenue provided by battery installation is normalized against the results obtained knowing the prices in advance, which represent the best achievable improvement. This is represented through a prediction efficiency defined as

$$\eta_{pred} = \frac{R_{opt} - R_{base}}{R_{best} - R_{base}}, \tag{19}$$

where a unitary efficiency η_{pred} indicates that the price predicting algorithms in the loop provide hourly prices r_i which are accurate enough to always find the best scheduling for the following day.

As cycling a battery contributes to its degradation, it is important to compare the additional revenue against the total energy exchanged during the observation period. This is done by metric ρ, defined as

$$\rho = \frac{R_{increase}}{\int (P_{ch} + P_{dch})dt} \tag{20}$$

which provides a revenue in €/MWh, measuring how profitably the system is cycled.

Finally, a key metric for evaluating profitability of an installation is the return on investment (ROI), defined as the ratio between the revenues and the investments. For the evaluations to be conducted in this project, the investment considers the purchase cost of batteries, as they are the main difference between the first life system and the one assembled from second life modules. Therefore, ROI is defined as

$$ROI = \frac{R_{increase} - Cost_{aux}}{Cost_{batt}}. \tag{21}$$

$Cost_{aux}$ is the yearly expense for BESS functioning, which includes necessary container conditioning and energy consumption by monitoring and communication systems. On the other hand, $Cost_{batt}$ is not limited to battery purchase cost, but it also includes module transport to the site and their re-collection at the end of the second life, since manufacturers perform recycling themselves. This strategic decision by battery providers has the goal to progressively increase the share of recycled raw material in compliance with European Union targets to be met by 2031 [86].

3. Case study

The described methodology has been developed during the conduction of the project BESS-2L, aimed at realizing a stationary battery storage system in support of a hydroelectric power plant operated by Compagnia Valdostana Acque (CVA) in Aosta Valley, shown in Fig. 3.

The main novelty of the project is the mixed utilization of fresh batteries designed for stationary applications and exhausted batteries from vehicular applications,sourced directly from the EV manufacturer, which certified that all modules have a SoH of 80% (± 1%). This particular structure, shown in Fig. 4, required the conduction of experimental tests aimed at assessing η_{RTE} of the second life component with respect to the first life one. These on-field tests validate BESS installation for a generic power plant, as coupling is conducted at the 6 kV busbar (where POD is located) and is independent from the energy source. This generalized experimental validation is necessary for economical evaluations, as it allows to simulate different BESS sizes as well as their application to other plants.

The two subsystems have similar capacity, but different chemistries and connections to the distribution grid. The first life subsystem is built from LFP batteries and is connected directly to the AC/DC converter for interaction with the distribution network; the second life subsystem is built assembling NCM modules recycled from automotive application and must operate at a lower voltage. As can be seen from Fig. 4, a DC/DC buck–boost converter is needed for the second life subsystem. Although this impacts its total η_{RTE}, application of such a converter is a common feature in literature, due to the unbalances that their different first life usage profiles can generate [87–91]. Both the first life and the second life subsystem feed an inverter which outputs a voltage level of 470 V, regardless of SoC changes, as shown in Fig. 4. Low level controls impose the current to or from each subsystem in order to achieve the desired total power flow, while minimizing SoC unbalances.

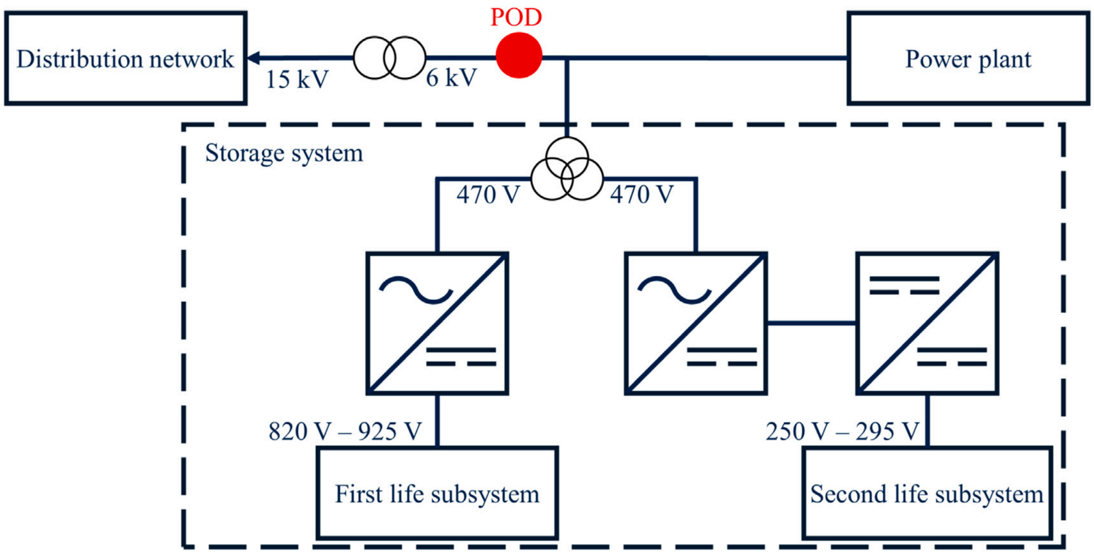

Fig. 4. Structure of energy storage system from BESS-2L project.

Each of the subsystems is located inside a closed container, whose room temperature is kept around 25 °C, regardless of the external weather conditions. This is fundamental to ensure system safety and to prevent thermal runaways which would be catastrophic for utility-scale installations such as this [92–94]. Thermal management is performed by means of forced ventilation alone, following the most common solutions employed in stationary storage systems [44]. Its main advantages are simplicity and reduced costs with respect to a liquid cooling circuit. Extension of air cooling to the subsystem realized from automotive modules instead of liquid cooling is justified by the less demanding usage profile compared to their first life application [79].

3.1. Power plants under study

3.1.1. Hydroelectric power plant

The plant on which the project was conducted is a free-flow hydroelectric power plant operated by CVA in Valle d'Aosta. Its selection as a testbed for the application of static accumulators is dictated by its non-programmable nature. While the largest hydroelectric solutions are basin-regulated and their production is controlled, the selected plant is free-flow and its production cannot be programmed to cope with demand peaks. Therefore, it is an example of electricity generation from NP-RES, which benefits the most from application of batteries for energy arbitration. The maximum power coming from the turbines is around 88% of the total plant output allowed by transformers. The power rating of AC/DC converters used to link the stationary accumulator system to the hydraulic turbines is 84% of batteries nominal capacity, thus imposing a stricter limit to charge and discharge operations, which cannot be performed at 1C. Therefore, Inequalities (8) and (9) are modified as in (22) and (23).

$$P_{ch,i} \leq 0.84\frac{C_{batt}}{1h} \cdot \frac{1}{\sqrt{\eta_{RTE}}}, \quad \forall i \in \{1, 2 \ldots N_{hours}\} \tag{22}$$

$$P_{dch,i} \leq 0.84\frac{C_{batt}}{1h} \cdot \sqrt{\eta_{RTE}}, \quad \forall i \in \{1, 2 \ldots N_{hours}\} \tag{23}$$

3.1.2. Photovoltaic power plant

To obtain a complete picture of arbitrage profitability, further studies were conducted extending the application of the accumulation system to another power plant based on NP-RES operated by CVA, a photovoltaic park located in northern Italy. Considerations on such a plant are relevant for the evaluation of stationary accumulating systems impacts, as their hours of maximum output are those with the lowest price throughout the day, as seen in Fig. 5. The maximum electric output generation from solar panels P_{plant} is equal to the nominal power rating P_{max} allowed by converters linking the plant to electricity transmission network. This does not represent an issue in terms of operation scheduling, as battery discharge never takes place during photovoltaic output hours, unlike what happens in hydroelectric plants. The additional constraint represented by AC/DC converters power rating is kept at 84% of battery capacity, the same as the hydroelectric power plant, to perform a meaningful comparison.

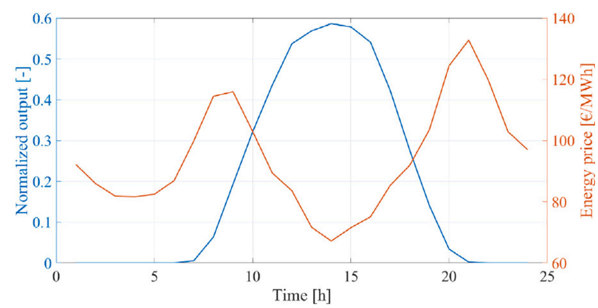

Fig. 5. Comparison of photovoltaic output and electricity price. Average May 2024.

3.1.3. Multi-site installation and temperature impact on profitability

Experimental results of BESS-2L project have been used to perform economic evaluations, assessing the impact of BESS installation on the profitability of a hydroelectric power plant and on a photovoltaic park. The two analyzed facilities are located in Northern Italy, therefore their operating conditions are similar (C_{aux} is 1000 €/MWh yearly), but future work could be conducted replicating the activities of BESS-2L project in another of the plants operated by CVA, which are shown in Fig. 6. In particular, application of batteries to the wind farms located in Southern Italy would be beneficial to evaluate the impact of local climate on container conditioning costs included in C_{aux}, balancing them against the impact of higher room temperature on η_{RTE} and degradation speed. Furthermore, these plants belong to another electrical sub-zone, whose negotiations are conducted separately, leading to slightly different prices (~ 1% yearly), although grid regulations are the same.

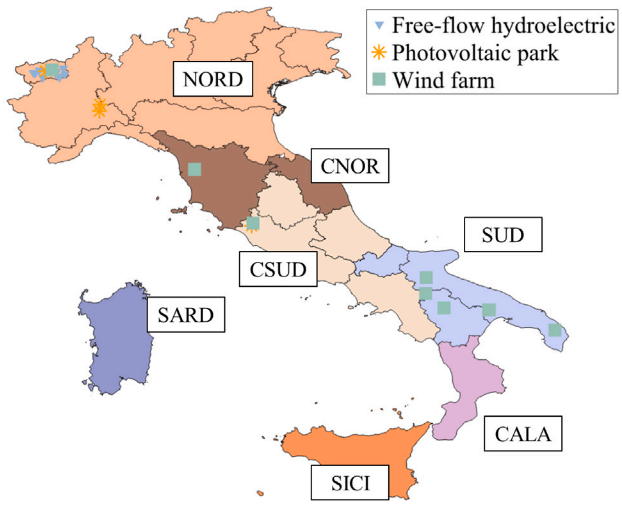

Fig. 6. Power plants based on NP-RES operated by CVA, spread across four of the seven Italian electrical sub-zones.

3.2. Round-trip efficiency tests

To evaluate the impact of second life batteries on total plant revenues, RTE tests were performed on the two subsystems separately during the second half of June 2024. All modules were installed in the respective containers, which were closed, since system operation is always conducted remotely. Air conditioning was active at all times, keeping room temperature at 25 °C through forced ventilation, while the external values fluctuated between 30 °C and 35 °C. Testing was conducted according to the following steps: (1) SoC was calibrated by bringing it to the minimum level permitted by the BMS and allowed to rest; (2) the battery was charged in CP mode until the start of Constant Voltage (CV) mode, to simulate the operation during energy arbitration; (3) the system was rested for 75 min to allow cooling and electrical relaxation. Such a pause is only 30% of the rest imposed during daily operation and, therefore, it represents a significantly harsher operation than what is imposed in reality; (4) the battery system was discharged in CP mode and brought back to the SoC obtained at the end of point 1 to complete a full charge and discharge cycle. The total energy absorbed and released by the system was measured at the POD of the power plant (Fig. 4), therefore the η_{RTE} obtained from these tests also accounts for all losses through inverter stages.

3.3. Second life cells experimental characterization

To assemble a second life stationary accumulator, it is necessary to assess the quality of the cells recycled from automotive usage through experimental testing. The process was conducted inside a laboratory with air conditioning aimed at keeping room temperature at 25 °C, to replicate the operating conditions of the battery system inside the container. Current and voltage profiles were provided through a "ITECH IT6015C-80-450" bidirectional DC power supply. The goals of such activity are: (a) identifying the remaining usable capacity for system dimensioning; (b) obtaining the curves of open circuit voltage and internal resistance as a function of SoC, fundamental information for the realization of a BMS to keep the assembly balanced. To assess (a), charge and discharge cycles were imposed to the cell. Discharge was conducted in Constant Current (CC) mode, while all charges were performed in CC–CV mode. First, a capacity test at low current was conducted at $C_{cell}/5$, where cell capacity C_{cell} is obtained from that of the module when new C_{mod} via the number of parallel cells N_{par} as

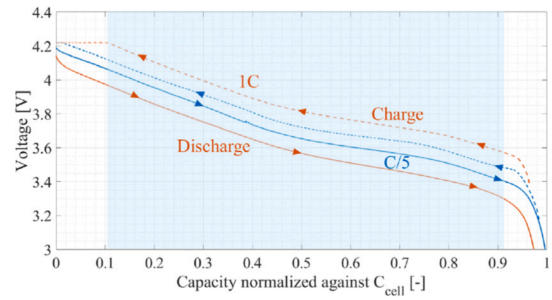

Fig. 7. Capacity tests conducted on the second life cell. The shaded area represents the on-field operating conditions of the cell, in CP charge and discharge between 4.22 V and 3.3 V.

in Eq. (24). The cell was cycled between 2.9 V and 4.22 V, with CV phase ending when the current dropped below $C_{cell}/10$.

$$C_{cell} = \frac{C_{mod}}{N_{par}} \tag{24}$$

The next step was performing the capacity test at nominal rate to assess cyclability in the conditions imposed by stationary storage operation. The cell was cycled at C_{cell} between 2.9 V and 4.22 V, with CV phase ending when the current dropped below $C_{cell}/10$. The results of the capacity tests are shown in Fig. 7. Increasing the C-rate from $C_{cell}/5$ to $1C_{cell}$ does not vary significantly the total capacity extracted, indicating that the cell under test is suitable for execution of full charge in an hour, in accordance with the operating strategy defined to maximize profit. The shaded area of Fig. 7 represents the operating interval in which the module BMS allows the cell to operate at $1C_{cell}$, as module voltage is constrained between $3.3N_{series}$ V and $4.22N_{series}$ V from datasheet.

The second test campaign conducted on the cell was aimed at extracting (b) the open circuit voltage and internal resistance as a function of SoC. To do so, the cell was discharged by 5% of the total capacity obtained during the first test campaign, and then allowed to rest for 12 min. Once it was fully discharged, the same procedure was repeated in charge. Last steps of charge and discharge procedures have been slightly adjusted to satisfy the constraints of minimum and maximum voltage. The voltage at the end of each relaxation phase, highlighted by circles in Fig. 8, is taken as the V_{OC} for the corresponding level of SoC, as shown in Fig. 9a. It is shown that the curves of OCV after relaxation measured in charge and discharge overlap significantly, demonstrating that 12 min of rest allow for full recovery of OCV from the excited state. On the other hand, the internal resistance demonstrates two opposite trends in charge and discharge. The value of R_{int} was obtained comparing the curves obtained from the capacity test of Fig. 7 V_{batt} with the open circuit voltage V_{OC} as in Eq. (25).

$$R_{int} = \frac{V_{batt} - V_{OC}}{I} \tag{25}$$

During discharge at high SoC, the cell is characterized by a very low R_{int}, which instead reaches the maximum for discharge at low SoC, a commonly observed phenomenon [95]. The opposite trend is noted for R_{int} during charge, with high values observed over 90% SoC, due to CV operation instead of CC. With the exception of the peaks in extreme SoC conditions, the obtained R_{int} in the operating region of the cell, described by the shaded region of Fig. 9, is oscillating around values that are between 38 and 50% of the maximum resistance, a behavior similar to what is found in previous literature [96].

3.4. Revenue estimation

To conduct economic evaluations on the usage of first or second life battery modules, it is necessary to evaluate the performance of the system on a sufficiently long period of time. This is necessary to

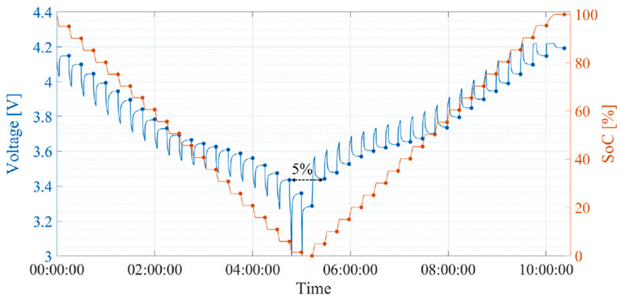

Fig. 8. Testing procedure to extract second life cell OCV. Circles highlight values of V and SoC taken at the end of the relaxation. In particular, the two points corresponding to 5% SoC are highlighted.

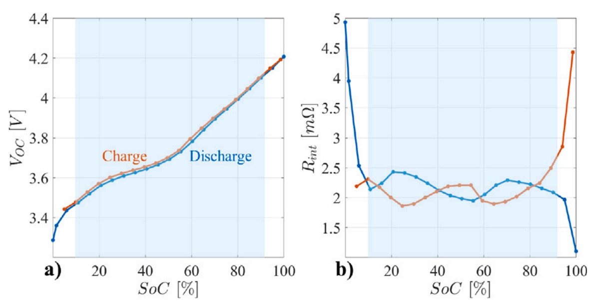

Fig. 9. Results from open circuit voltage tests. Shaded area represents the on-field operating region of the cell. **a)** Open Circuit Voltage V_{OC} after 12 min of rest as a function of SoC. **b)** Internal resistance R_{int} as a function of SoC.

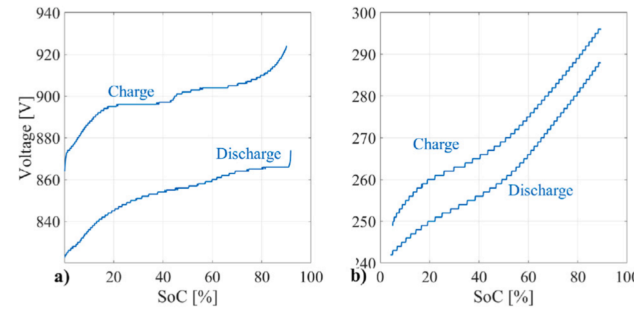

Fig. 10. Voltage trend during RTE tests. **a)** First life subsystem. **b)** Second life subsystem.

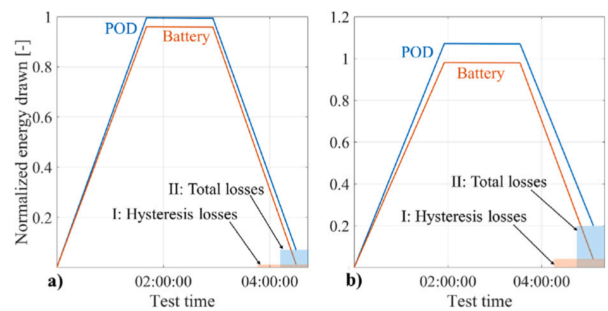

Fig. 11. Net energy drawn from the grid during RTE tests. **a)** First life subsystem. **b)** Second life subsystem.

filter out the seasonal trends in electricity production, caused by lower sunshine or reduced river flow. For this case study, the considered time window is the year 2023, to capture production trends and seasonal price variations.

The system composed of battery and power plant was modeled in Matlab Simulink environment and its operation through the year was simulated to assess the revenues for different installed capacities and RTEs. Day-ahead scheduling of battery operation was represented via the generation of a price database to forecast price trends. This was used to test the control logics, which define charge and discharge based on past days and receive information about prices only after communicating the schedule. In parallel, a second plant is simulated, with full knowledge of electricity prices, to assess the best possible profit granted by energy arbitration. The comparison between these two results is fundamental in tuning the price prediction function, as it points out the missed revenues due to poor forecasting accuracy.

The two plants also include a simplified degradation model to obtain realistic results. While C_{batt} is a constant in the daily optimization problem, the value fed to the programming algorithm is recomputed for each iteration. Degradation is represented through a reduction of the installed capacity which occurs constantly everyday with a total decrease of 1.5% at the end of the year. This drop is a conservative estimate, adapted from previous experiments in literature, which see a yearly degradation around 3% performing 4.5 equivalent full charge–discharge cycles in a day [81].

4. Results

4.1. Round-trip efficiency tests

Round-trip efficiency tests were conducted separately on the first life and on the second life subsystems, by mean of charge and discharge tests operated in CP at a power corresponding to 60% of the installed capacity C_{plant}, that is

$$P_{ch} = P_{dch} = 0.6\frac{C_{plant}}{1h} \tag{26}$$

This operation mode is the one that best represents daily operation, as P_{max} and P_{plant} constrain the battery to work at C-rates below the limits imposed by the inverter and, over the entire 2023 simulations, the average of P_{ch} and P_{dch} was 60% of the one corresponding to 1 h discharge. The constant power applied was measured at the POD, so that the resulting efficiency is consistent with system operation.

The results of RTE tests conducted on the first life subsystem are shown in Figs. 10a and 11a. The BMS allowed CP discharge until the lower operation limit, as shown by the 0% SoC in Fig. 10a. Charge was interrupted as soon as the CP phase ended, around 90% SoC. Fig. 11b displays the energy drawn from the grid to be stored in the battery. The blue curve refers to the value obtained from integration of the power as measured at the POD, while the orange one considers the power measured at battery level. In total, the energy that the subsystem inserts in the network during discharge is lower than that drawn during charge by around 7%. Part of this is due to hysteresis losses caused by overvoltages and undervoltages, highlighted by area I in Fig. 11a. However, most of the total losses (area II) take place at the inverter stage, as the charge–discharge efficiency of the battery alone η_{batt} amounts to 98%, while overall efficiency η_{RTE} for the first life subsystem amounts to 92.9%.

Results of RTE tests conducted on the subsystem assembled from second life automotive batteries are displayed in Figs. 10b and 11b. The voltage-SoC curve obtained from tests on the entire subsystem is in agreement with the OCV curve obtained during laboratory test on a single cell. As with the first life subsystem, CP charging ended around 90% SoC. However, the BMS in charge of balancing the second life modules did not allow for CP discharge until the lower operating limit, stopping it at 5%. From the comparison between Fig. 11a and 11b, it is evident that the second life subsystem experiences larger losses during

Table 1
Efficiency comparison of 1st and 2nd life storage systems, from experimental tests.

1st life system		2nd life system	
η_{batt}	η_{RTE}	η_{batt}	η_{RTE}
98%	92.9%	97%	81.3%

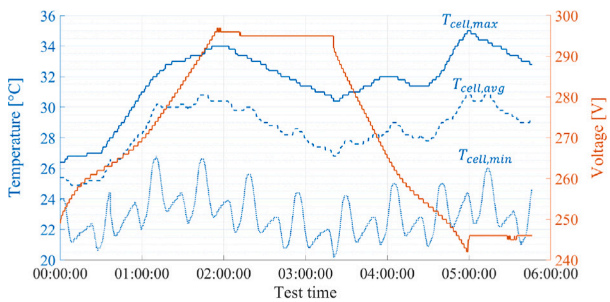

Fig. 12. Trend of temperature during the RTE test of second life subsystem.

a whole charge–discharge cycle. This is partly due to an increase of the hysteresis losses (I), a common phenomenon for aged batteries [97]. Battery efficiency η_{batt} drops from 98% to 97%, but the majority of the increase derives from the necessary introduction of the DC/DC converter between the battery and the inverter. Overall, η_{RTE} for the second life subsystem is 81.3%. The round-trip efficiency of each of the subsystems and the charge–discharge efficiency of the battery itself are presented in Table 1.

In addition to efficiency identification, capacity tests conducted on the second life subsystem also allowed to evaluate the suitability of the forced air solution in place of liquid cooling, as shown by Fig. 12. It can be seen that the average temperature of the cells exceeds 30 °C only at the end of the charge and discharge phases, when the battery has been working for almost two hours. In addition to this, the highest logged cell temperature is 35 °C and the difference between average and maximum reaches a peak of 4.5 °C in correspondence of the end of discharge phase. These results show a satisfactory balance of cell temperature during real operation, ensuring that none of the components move out of the region for normal battery operation [98]. Therefore, capacity tests demonstrated that forced ventilation cooling is applicable also to the second life modules which were designed for liquid cooling.

4.2. Economic results

Fig. 13 shows the yearly revenue increase $R_{inc,pct}$ (Eq. (18)) for the application of a stationary accumulation system as a function of the installed capacity. The difference in trend between a) and b) is evident. For the free-flow hydroelectric plant, the increase in revenue exhibits a less than linear increase with respect to battery capacity, due to the seasonal trends in energy production, which cause low values of P_{plant} at the beginning of the year. However, limitations imposed by transformer power rating P_{max} are relevant as well, since they prevent from exploiting the maximum discharge power in the most remunerative hours. On the contrary, profitability increase for the PV plant is linear for capacities below 80% of the nominal plant power. Since the most remunerative hours have no electricity generation, P_{plant} does not force the accumulator to discharge at lower rates. On the other hand, maximum production timeslots correspond to the least remunerative hours. Therefore, in PV application, the battery can always fully exploit the price difference between daily minimum and maximum.

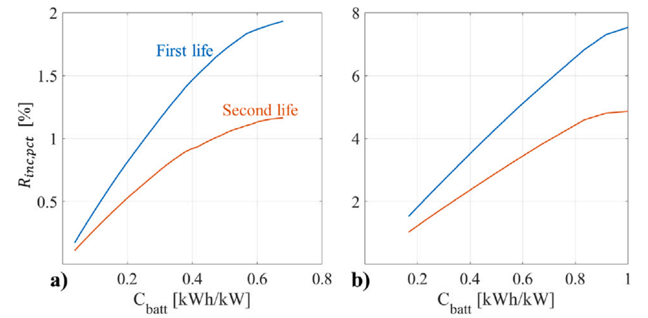

Fig. 13. Yearly revenue increase $R_{inc,pct}$ as a function of installed capacity normalized against plant output. a) Free-flow hydroelectric power plant. b) Photovoltaic park.

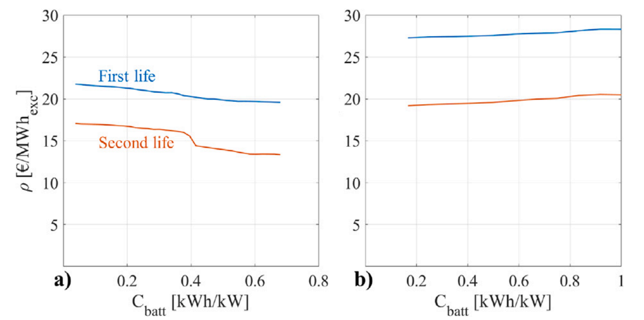

Fig. 14. Specific revenue ρ as a function of installed capacity normalized against plant output for first and second life batteries. a) Free-flow hydroelectric power plant. b) Photovoltaic park.

The aforementioned characteristics of energy market and plant output also impact the trends of specific revenue ρ as a function of storage size, as shown in Fig. 14. Increasing the installed capacity in a free-flow hydroelectric power plants reduces ρ linearly. This is caused by P_{max} limitations, which prevent from discharging during the hour with maximum price, therefore imposing to operate the batteries in a less efficient way. The significant drop for second life storage sizes above 40% of the hydroelectric plant maximum hourly output is caused by the relation between maximum turbines output and maximum power plant output, with the former being around 88% of the latter. As a consequence, during spring time, when P_{plant} is at its maximum, batteries specific revenues drop, and this is more evident for second life modules, where a larger part of exchanged energy is lost due to lower η_{RTE}. On the other hand, ρ increases minimally with larger installed capacities for PV plants. The reason for the increase comes from the fact that the days with the highest peak solar production to be exploited are those with the largest difference between minimum and maximum prices. Therefore, a larger battery can take more advantage of days with the highest sunshine, causing the minimal increase seen in Fig. 14b.

The better performances in terms of $R_{inc,pct}$ and ρ for the PV installation are due to the differences in plant operating conditions rather than accuracy of price prediction logics. This can be seen from Fig. 15, which compares the values of η_{pred} for the two types of plant. In both cases, battery usage scheduling performed without prior knowledge of price profiles yields satisfactory results, with revenues granted by energy arbitration in the region of 90% of the maximum achievable results for first life accumulators and around 80% for re-used automotive modules. The lower result for the second life case is a consequence of the reduced η_{RTE}, which causes the system to absorb more energy and release less in the grid, making it more impacted by mismatches between predictions and real prices.

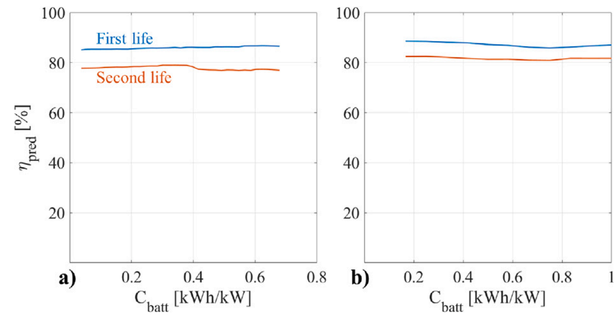

Fig. 15. Prediction efficiency η_{pred} as a function of installed capacity normalized against plant output. a) Free-flow hydroelectric power plant for first and second life batteries. b) Photovoltaic park.

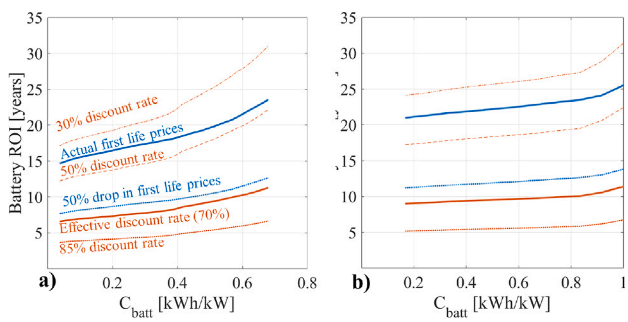

Fig. 16. ROI as a function of installed capacity normalized against plant output and for different discount rates on second life batteries (red curves). a) Free-flow hydroelectric power plant. b) Photovoltaic park. (For interpretation of the references to color in this figure legend, the reader is referred to the web version of this article.)

Despite the worse performances with respect to the solar park, the application to hydroelectric power plant shows a faster ROI for the purchase of batteries for energy arbitration, as shown in Fig. 16. This happens because, although with lower efficiency, the hydroelectric power plant exploits the batteries more, with the execution of two charges and discharges a day, compared to the single cycle that can be performed in the PV plant. Therefore, as can be seen from comparing Fig. 16a and b, the ratio between battery cost and yearly profit is lower for the hydroelectric plant, indicating a faster payback.

Most importantly, the study conducted on the basis of real experimental η_{RTE}, power production data and electricity cost highlights that payback is considerably faster for the installation of second life modules. This is because batteries recovered after automotive usage were purchased at a price that is 70% cheaper in €/kWh than what was paid for the fresh LFP modules. Although battery prices are following a downwards trend, Fig. 16 shows that first life accumulator prices should fall by over 50% to outperform the ROI offered by second life batteries with the same discount rate experienced in the project. On the other hand, enforcement of regulations on exhausted traction modules might generate a larger flow of second life batteries dismantled from vehicles, driving down their prices. Overall, Fig. 16 shows that discount rates as low as 50% are enough to keep second life more profitable than first life batteries at current prices while, on the opposite side, with a price reduced by 85%, second life batteries would require only 5 years to pay back the investment.

5. Conclusions

This article presented an economical analysis drawn from the results of the BESS-2L project. In this context, a stationary energy storage system was realized integrating fresh batteries for building applications with an equally sized assembly of re-used second life modules from vehicular applications. Experimental tests demonstrated the feasibility of such a system, with the second life subsystem able to deliver constant power during a full charge–discharge cycle at 60% of its nominal power in the same way as the first life one. During these tests, it was also proved that ventilation cooling is sufficient even for modules designed for liquid cooling, like automotive ones, thanks to the less demanding usage profile.

The necessary presence of one additional DC/DC conversion stage in the second life portion of the stationary storage impacted its η_{RTE}, which drops from 92.9% to 81.3%. However, through analysis of one year of real plant production programs and energy price on the national exchange, it was demonstrated that even with a lower efficiency, re-used batteries are able to provide a profitability increase for power plants based on NP-RES, up to 1.2% for hydroelectric generation and 5% for solar parks. These results also show that, despite having a smaller impact on plant profitability overall, battery payback is faster in the case of free-flow hydroelectric power plants than for photovoltaic, as their production program allows to exploit the storage system more, through the execution of two cycles a day.

Most importantly, it was demonstrated that second life modules offer a payback that is twice as fast compared to first life systems, thanks to a purchase price that is over 70% lower, but they would remain competitive even if the discount dropped to 50%. This cost advantage is bound to increase in the coming years, as the expansion of EV diffusion will increase the demand for fresh batteries, while the offer of used modules will inevitably ramp up, as a consequence of the growth of electric mobility in the past decade. Therefore, the installation of second life battery modules, that this article proved as economically advantageous already, will steadily become more profitable than first life installations. At the same time, second life energy storage solutions will improve the entire electric mobility life cycle, reducing its waste in landfills and improving the efficiency of renewable electricity generation.

To conclude, this project has demonstrated the feasibility and profitability of installation of recycled batteries in renewable electricity production, a key step to make mobility electrification sustainable in all fields, economically and environmentally.

CRediT authorship contribution statement

Alberto Ponso: Writing – original draft, Software, Methodology, Investigation. **Eleonora Cerva:** Writing – review & editing, Methodology, Investigation. **Nicholas Monticone:** Writing – review & editing, Methodology, Investigation. **Rocco Sorace:** Writing – review & editing, Methodology, Investigation. **Angelo Bonfitto:** Writing – review & editing, Supervision, Methodology, Conceptualization. **Andrea Tonoli:** Writing – review & editing, Supervision, Methodology, Conceptualization.

Research support

The BESS-2L program was funded by Aosta Valley ERDF 2021–2027 Program.

Declaration of competing interest

The authors declare that they have no known competing financial interests or personal relationships that could have appeared to influence the work reported in this paper.

Acknowledgments

The research work was developed in the framework of the activities of the Interdepartmental Center for Automotive Research and Sustainable Mobility (CARS) at Politecnico di Torino (www.cars.polito.it).

Data availability

The data that has been used is confidential.

References

[1] M. Joshi, E. Hawkins, R. Sutton, J. Lowe, D. Frame, Projections of when temperature change will exceed 2 ° c above pre-industrial levels, Nat. Clim. Chang. 1 (8) (2011) 407–412, http://dx.doi.org/10.1038/nclimate1261.

[2] J. Hansen, M. Sato, R. Ruedy, K. Lo, D.W. Lea, M. Medina-Elizade, Global temperature change, Proc. Natl. Acad. Sci. 103 (39) (2006) 14288–14293, http://dx.doi.org/10.1073/pnas.0606291103.

[3] W. Steffen, P.J. Crutzen, J.R. McNeill, The anthropocene: are humans now overwhelming the great forces of nature? in: R.E. Dunn, L.J. Mitchell, K. Ward (Eds.), The New World History, University of California Press, 2019, pp. 440–459, http://dx.doi.org/10.1525/9780520964297-051.

[4] M. Crippa, D. Guizzardi, M. Banja, E. Solazzo, M. Muntean, E. Schaaf, F. Pagani, F. Monforti-Ferrario, J. Olivier, R. Quadrelli, A. Risquez Martin, P. Taghavi-Moharamli, G. Grassi, S. Rossi, D. Oom, A. Branco, J. San-Miguel, E. Vignati, CO2 emissions of all world countries: JRC/IEA/PBL 2022 report, JRC/IEA/PBL Report, European Commission. Joint Research Centre., LU, 2022.

[5] D. Ivanova, J. Barrett, D. Wiedenhofer, B. Macura, M. Callaghan, F. Creutzig, Quantifying the potential for climate change mitigation of consumption options, Environ. Res. Lett. 15 (9) (2020) 093001, http://dx.doi.org/10.1088/1748-9326/ab8589.

[6] Y. Oura, Y. Mochinaga, H. Nagasawa, Railway electric power feeding systems, Jpn. Railw. Transp. Rev. 16.10 (1998) 48–58.

[7] M.M. Thackeray, C. Wolverton, E.D. Isaacs, Electrical energy storage for transportation—approaching the limits of, and going beyond, lithium-ion batteries, Energy Environ. Sci. 5 (7) (2012) 7854, http://dx.doi.org/10.1039/c2ee21892e.

[8] T. Placke, R. Kloepsch, S. Dühnen, M. Winter, Lithium ion, lithium metal, and alternative rechargeable battery technologies: the odyssey for high energy density, J. Solid State Electrochem. 21 (7) (2017) 1939–1964, http://dx.doi.org/10.1007/s10008-017-3610-7.

[9] S. Hegde, L.M. Castellanos Molina, A. Bonfitto, R. Galluzzi, N. Amati, A. Tonoli, Crankshaft Decoupling Effects on Fuel Economy in HEV-P0, in: Volume 1: 24th International Conference on Advanced Vehicle Technologies (AVT), American Society of Mechanical Engineers, St. Louis, Missouri, USA, 2022, http://dx.doi.org/10.1115/DETC2022-90014, V001T01A016.

[10] P.G. Anselma, P.J. Kollmeyer, S. Feraco, A. Bonfitto, G. Belingardi, A. Emadi, N. Amati, A. Tonoli, Assessing Impact of Heavily Aged Batteries on Hybrid Electric Vehicle Fuel Economy and Drivability, in: 2021 IEEE Transportation Electrification Conference & Expo (ITEC), IEEE, Chicago, IL, USA, 2021, pp. 696–701, http://dx.doi.org/10.1109/ITEC51675.2021.9490149.

[11] A. Ponso, A. Bonfitto, G. Belingardi, Route Planning for Electric Vehicles Including Driving Style, HVAC, Payload and Battery Health, Energies 16 (12) (2023) 4627, http://dx.doi.org/10.3390/en16124627, URL https://www.mdpi.com/1996-1073/16/12/4627.

[12] A. Podias, A. Pfrang, F. Di Persio, A. Kriston, S. Bobba, F. Mathieux, M. Messagie, L. Boon-Brett, Sustainability Assessment of Second Use Applications of Automotive Batteries: Ageing of Li-Ion Battery Cells in Automotive and Grid-Scale Applications, World Electr. Veh. J. 9 (2) (2018) 24, http://dx.doi.org/10.3390/wevj9020024.

[13] L. Canals Casals, M. Rodríguez, C. Corchero, R.E. Carrillo, Evaluation of the End-of-Life of Electric Vehicle Batteries According to the State-of-Health, World Electr. Veh. J. 10 (4) (2019) 63, http://dx.doi.org/10.3390/wevj10040063.

[14] W. Diao, J. Kim, M.H. Azarian, M. Pecht, Degradation modes and mechanisms analysis of lithium-ion batteries with knee points, Electrochim. Acta 431 (2022) 141143, http://dx.doi.org/10.1016/j.electacta.2022.141143.

[15] S. Klein, P. Bärmann, L. Stolz, K. Borzutzki, J.-P. Schmiegel, M. Börner, M. Winter, T. Placke, J. Kasnatscheew, Demonstrating Apparently Inconspicuous but Sensitive Impacts on the Rollover Failure of Lithium-Ion Batteries at a High Voltage, ACS Appl. Mater. & Interfaces 13 (48) (2021) 57241–57251, http://dx.doi.org/10.1021/acsami.1c17408.

[16] P.M. Attia, A. Bills, F. Brosa Planella, P. Dechent, G. Dos Reis, M. Dubarry, P. Gasper, R. Gilchrist, S. Greenbank, D. Howey, O. Liu, E. Khoo, Y. Preger, A. Soni, S. Sripad, A.G. Stefanopoulou, V. Sulzer, Review—"Knees" in Lithium-Ion Battery Aging Trajectories, J. Electrochem. Soc. 169 (6) (2022) 060517, http://dx.doi.org/10.1149/1945-7111/ac6d13.

[17] W. Gao, Z. Cao, Y. Fu, C. Turchiano, N.V. Kurdkandi, J. Gu, C. Mi, Comprehensive study of the aging knee and second-life potential of the Nissan Leaf e+ batteries, J. Power Sources 613 (2024) 234884, http://dx.doi.org/10.1016/j.jpowsour.2024.234884.

[18] P. Fermín-Cueto, E. McTurk, M. Allerhand, E. Medina-Lopez, M.F. Anjos, J. Sylvester, G. Dos Reis, Identification and machine learning prediction of knee-point and knee-onset in capacity degradation curves of lithium-ion cells, Energy AI 1 (2020) 100006, http://dx.doi.org/10.1016/j.egyai.2020.100006.

[19] H. Zhang, F. Altaf, T. Wik, Battery capacity knee-onset identification and early prediction using degradation curvature, J. Power Sources 608 (2024) 234619, http://dx.doi.org/10.1016/j.jpowsour.2024.234619.

[20] M. Fuhrmann, L. Torcheux, Y. Kobayashi, Knee point prediction for lithium-ion batteries using differential voltage analysis and degree of inhomogeneity, J. Power Sources 621 (2024) 235210, http://dx.doi.org/10.1016/j.jpowsour.2024.235210.

[21] T. Wang, Y. Zhu, W. Zhao, Y. Gong, Z. Zhang, W. Gao, Y. Shang, Capacity degradation analysis and knee point prediction for lithium-ion batteries, Green Energy Intell. Transp. 3 (5) (2024) 100171, http://dx.doi.org/10.1016/j.geits.2024.100171.

[22] D. Fang, W. Wu, J. Li, W. Yuan, T. Liu, C. Dai, Z. Wang, M. Zhao, Performance simulation method and state of health estimation for lithium-ion batteries based on aging-effect coupling model, Green Energy Intell. Transp. 2 (3) (2023) 100082, http://dx.doi.org/10.1016/j.geits.2023.100082.

[23] H. Tang, Y. Wu, Y. Cai, F. Wang, Z. Lin, Y. Pei, Design of power lithium battery management system based on digital twin, J. Energy Storage 47 (2022) 103679, http://dx.doi.org/10.1016/j.est.2021.103679.

[24] W. Li, M. Rentemeister, J. Badeda, D. Jöst, D. Schulte, D.U. Sauer, Digital twin for battery systems: Cloud battery management system with online state-of-charge and state-of-health estimation, J. Energy Storage 30 (2020) 101557, http://dx.doi.org/10.1016/j.est.2020.101557.

[25] J. Song, W. Yan, H. Cao, Q. Song, H. Ding, Z. Lv, Y. Zhang, Z. Sun, Material flow analysis on critical raw materials of lithium-ion batteries in China, J. Clean. Prod. 215 (2019) 570–581, http://dx.doi.org/10.1016/j.jclepro.2019.01.081.

[26] IEA, Trends in batteries, Tech. rep., International Energy Agency, Paris, 2023.

[27] M. Bruno, S. Fiore, Review of lithium-ion batteries' supply-chain in Europe: Material flow analysis and environmental assessment, J. Environ. Manag. 358 (2024) 120758, http://dx.doi.org/10.1016/j.jenvman.2024.120758.

[28] J. Figgener, P. Stenzel, K.-P. Kairies, J. Linßen, D. Haberschusz, O. Wessels, G. Angenendt, M. Robinius, D. Stolten, D.U. Sauer, The development of stationary battery storage systems in Germany – a market review, J. Energy Storage 29 (2020) 101153, http://dx.doi.org/10.1016/j.est.2019.101153.

[29] A. Saldarini, M. Longo, M. Brenna, D. Zaninelli, Battery Electric Storage Systems: Advances, Challenges, and Market Trends, Energies 16 (22) (2023) 7566, http://dx.doi.org/10.3390/en16227566.

[30] Y.-R. Lee, H.-J. Kang, M.-K. Kim, Optimal Operation Approach With Combined BESS Sizing and PV Generation in Microgrid, IEEE Access 10 (2022) 27453–27466, http://dx.doi.org/10.1109/ACCESS.2022.3157294.

[31] E. O'Shaughnessy, J.R. Cruce, K. Xu, Too much of a good thing? Global trends in the curtailment of solar PV, Sol. Energy 208 (2020) 1068–1077, http://dx.doi.org/10.1016/j.solener.2020.08.075.

[32] R. Frank, Review and Growth Prospects of Renewable Energy in Luxembourg: Towards a Carbon-Neutral Future, in: 2024 4th International Conference on Smart Grid and Renewable Energy (SGRE), IEEE, Doha, Qatar, 2024, pp. 1–6, http://dx.doi.org/10.1109/SGRE59715.2024.10428765.

[33] A.A. Chien, L. Lin, As Grids Reach 100% Renewable at Peak, Growing Curtailment of 8 Gigawatts Looms as a Challenge to Decarbonization, ACM SIGEnergy Energy Informatics Rev. 4 (1) (2024) 3–10, http://dx.doi.org/10.1145/3649432.3649434.

[34] T. Brown, L. Reichenberg, Decreasing market value of variable renewables can be avoided by policy action, Energy Econ. 100 (2021) 105354, http://dx.doi.org/10.1016/j.eneco.2021.105354.

[35] L. Hirth, The market value of variable renewables, Energy Econ. 38 (2013) 218–236, http://dx.doi.org/10.1016/j.eneco.2013.02.004.

[36] C. Stiewe, A.L. Xu, A. Eicke, L. Hirth, Cross-border cannibalization: Spillover effects of wind and solar energy on interconnected European electricity markets, Energy Econ. 143 (2025) 108251, http://dx.doi.org/10.1016/j.eneco.2025.108251.

[37] IEA, Electricity Mid-Year Update 2025, Tech. rep., International Energy Agency, Paris, 2025.

[38] J. Wu, S. Powell, Y. Xu, R. Rajagopal, M.C. Gonzalez, Planning charging stations for 2050 to support flexible electric vehicle demand considering individual mobility patterns, Cell Rep. Sustain. 1 (1) (2024) 100006, http://dx.doi.org/10.1016/j.crsus.2023.100006.

[39] T. Mercier, M. Olivier, E. De Jaeger, The value of electricity storage arbitrage on day-ahead markets across Europe, Energy Econ. 123 (2023) 106721, http://dx.doi.org/10.1016/j.eneco.2023.106721.

[40] A.T. Veenstra, M. Mulder, Profitability of batteries in day-ahead and intraday electricity markets: Assessment of operation strategies with endogenous prices, Energy Econ. 148 (2025) 108608, http://dx.doi.org/10.1016/j.eneco.2025.108608.

[41] R.A. Campos, M. Braga, L. Nascimento, R. Ruther, G. Simoes, The Role of Second Life Li-ion Batteries in Avoiding Generation Curtailment in Utility-scale Wind + Solar Parks in Brazil, in: 2019 IEEE 46th Photovoltaic Specialists Conference (PVSC), IEEE, Chicago, IL, USA, 2019, pp. 2078–2081, http://dx.doi.org/10.1109/PVSC40753.2019.8980869.

[42] M. Weiss, K.C. Cloos, E. Helmers, Energy efficiency trade-offs in small to large electric vehicles, Environ. Sci. Eur. 32 (1) (2020) 46, http://dx.doi.org/10.1186/s12302-020-00307-8.

[43] E. Tramacere, S. Favelli, R. Manca, R. Galluzzi, A. Tonoli, Meeting Multiple Driving Needs: Design of a Novel Low Voltage Reconfigurable Electric Vehicle, in: 2024 IEEE Vehicle Power and Propulsion Conference (VPPC), IEEE, Washington, DC, USA, 2024, pp. 1–6, http://dx.doi.org/10.1109/VPPC63154.2024.10755297, https://ieeexplore.ieee.org/document/10755297/.

[44] H. Hesse, M. Schimpe, D. Kucevic, A. Jossen, Lithium-Ion Battery Storage for the Grid—A Review of Stationary Battery Storage System Design Tailored for Applications in Modern Power Grids, Energies 10 (12) (2017) 2107, http://dx.doi.org/10.3390/en10122107.

[45] D. Kucevic, B. Tepe, S. Englberger, A. Parlikar, M. Mühlbauer, O. Bohlen, A. Jossen, H. Hesse, Standard battery energy storage system profiles: Analysis of various applications for stationary energy storage systems using a holistic simulation framework, J. Energy Storage 28 (2020) 101077, http://dx.doi.org/10.1016/j.est.2019.101077.

[46] W. Mrozik, M.A. Rajaeifar, O. Heidrich, P. Christensen, Environmental impacts, pollution sources and pathways of spent lithium-ion batteries, Energy Environ. Sci. 14 (12) (2021) 6099–6121, http://dx.doi.org/10.1039/D1EE00691F.

[47] K.M. Winslow, S.J. Laux, T.G. Townsend, A review on the growing concern and potential management strategies of waste lithium-ion batteries, Resour. Conserv. Recycl. 129 (2018) 263–277, http://dx.doi.org/10.1016/j.resconrec.2017.11.001.

[48] M. Slattery, J. Dunn, A. Kendall, Transportation of electric vehicle lithium-ion batteries at end-of-life: A literature review, Resour. Conserv. Recycl. 174 (2021) 105755, http://dx.doi.org/10.1016/j.resconrec.2021.105755.

[49] J. Dunn, A. Kendall, M. Slattery, Electric vehicle lithium-ion battery recycled content standards for the US – targets, costs, and environmental impacts, Resour. Conserv. Recycl. 185 (2022) 106488, http://dx.doi.org/10.1016/j.resconrec.2022.106488.

[50] L. Canals Casals, M. Barbero, C. Corchero, Reused second life batteries for aggregated demand response services, J. Clean. Prod. 212 (2019) 99–108, http://dx.doi.org/10.1016/j.jclepro.2018.12.005.

[51] Q. Dong, S. Liang, J. Li, H.C. Kim, W. Shen, T.J. Wallington, Cost, energy, and carbon footprint benefits of second-life electric vehicle battery use, IScience 26 (7) (2023) 107195, http://dx.doi.org/10.1016/j.isci.2023.107195.

[52] H. Iqbal, S. Sarwar, D. Kirli, J.K.H. Shek, A.E. Kiprakis, A survey of second-life batteries based on techno-economic perspective and applications-based analysis, Carbon Neutrality 2 (1) (2023) 8, http://dx.doi.org/10.1007/s43979-023-00049-5.

[53] N. Fallah, C. Fitzpatrick, How will retired electric vehicle batteries perform in grid-based second-life applications? A comparative techno-economic evaluation of used batteries in different scenarios, J. Clean. Prod. 361 (2022) 132281, http://dx.doi.org/10.1016/j.jclepro.2022.132281, (Accessed 2025-10-02).

[54] Y. Cui, H.Y. Teah, Y. Dou, Y. Kanematsu, A. Yamaki, T. Yonetsuka, I.-S. Chang, J. Wu, Y. Kikuchi, Design and assessment of sustainable spent automobile lithium-ion battery industries in Japan: A system dynamic business model approach, J. Clean. Prod. 479 (2024) 144078, http://dx.doi.org/10.1016/j.jclepro.2024.144078.

[55] B. Faessler, Stationary, Second Use Battery Energy Storage Systems and Their Applications: A Research Review, Energies 14 (8) (2021) 2335, http://dx.doi.org/10.3390/en14082335.

[56] Japan Benex, Sumitomo Corp. to power plant with Nissan EVs, batteries, Tech. rep., Nissan Motor Corporation, 2018.

[57] A. Demirci, Optimal Sizing and Techno-Economic Evaluation of Microgrids Based on 100% Renewable Energy Powered by Second-Life Battery, IEEE Access 11 (2023) 113291–113306, http://dx.doi.org/10.1109/ACCESS.2023.3324547.

[58] M. Philippot, D. Costa, M.S. Hosen, A. Senécat, E. Brouwers, E. Nanini-Maury, J. Van Mierlo, M. Messagie, Environmental impact of the second life of an automotive battery: Reuse and repurpose based on ageing tests, J. Clean. Prod. 366 (2022) 132872, http://dx.doi.org/10.1016/j.jclepro.2022.132872.

[59] A. Ponso, A. Bonfitto, M. Silvagni, S. Luciani, Off-Board Testing Device for Battery Diagnostics and Market Analysis for Battery Reuse, in: Volume 1: 25th International Conference on Advanced Vehicle Technologies (AVT), American Society of Mechanical Engineers, Boston, Massachusetts, USA, 2023, http://dx.doi.org/10.1115/DETC2023-116596, V001T01A009.

[60] M.A. Cusenza, F. Guarino, S. Longo, M. Mistretta, M. Cellura, Reuse of electric vehicle batteries in buildings: An integrated load match analysis and life cycle assessment approach, Energy Build. 186 (2019) 339–354, http://dx.doi.org/10.1016/j.enbuild.2019.01.032.

[61] L. Colarullo, J. Thakur, Second-life EV batteries for stationary storage applications in Local Energy Communities, Renew. Sustain. Energy Rev. 169 (2022) 112913, http://dx.doi.org/10.1016/j.rser.2022.112913.

[62] J. Yan, Y. Yang, P. Elia Campana, J. He, City-level analysis of subsidy-free solar photovoltaic electricity price, profits and grid parity in China, Nat. Energy 4 (8) (2019) 709–717, http://dx.doi.org/10.1038/s41560-019-0441-z.

[63] G. Canestri, E. Cerva, F.D. Minuto, A. Lanzini, M. Moncecchi, M. Merlo, Renewable Energy Communities in Valle d'Aosta Region: development perspectives, in: 2021 IEEE 15th International Conference on Compatibility, Power Electronics and Power Engineering (CPE-POWERENG), IEEE, Florence, Italy, 2021, pp. 1–7, http://dx.doi.org/10.1109/CPE-POWERENG50821.2021.9501172.

[64] S.J. Tong, A. Same, M.A. Kootstra, J.W. Park, Off-grid photovoltaic vehicle charge using second life lithium batteries: An experimental and numerical investigation, Appl. Energy 104 (2013) 740–750, http://dx.doi.org/10.1016/j.apenergy.2012.11.046.

[65] L. Bartolucci, S. Cordiner, V. Mulone, M. Santarelli, F. Ortenzi, M. Pasquali, PV assisted electric vehicle charging station considering the integration of stationary first- or second-life battery storage, J. Clean. Prod. 383 (2023) 135426, http://dx.doi.org/10.1016/j.jclepro.2022.135426.

[66] J. Geng, S. Gao, X. Sun, Z. Liu, F. Zhao, H. Hao, Potential of electric vehicle batteries second use in energy storage systems: The case of China, Energy 253 (2022) 124159, http://dx.doi.org/10.1016/j.energy.2022.124159.

[67] Y. Deng, Y. Zhang, F. Luo, Y. Mu, Operational Planning of Centralized Charging Stations Utilizing Second-Life Battery Energy Storage Systems, IEEE Trans. Sustain. Energy 12 (1) (2021) 387–399, http://dx.doi.org/10.1109/TSTE.2020.3001015.

[68] G. Lacey, G. Putrus, A. Salim, The use of second life electric vehicle batteries for grid support, in: Eurocon 2013, IEEE, Zagreb, Croatia, 2013, pp. 1255–1261, http://dx.doi.org/10.1109/EUROCON.2013.6625141.

[69] H. Rallo, L. Canals Casals, D. De La Torre, R. Reinhardt, C. Marchante, B. Amante, Lithium-ion battery 2nd life used as a stationary energy storage system: Ageing and economic analysis in two real cases, J. Clean. Prod. 272 (2020) 122584, http://dx.doi.org/10.1016/j.jclepro.2020.122584.

[70] A. Fazeli, M. Stadie, M. Kerner, K. Poplavskaya, H. Nagaoka, J. Kapeller, J. Kathan, A. Burger, F. Jomrich, A Techno-economic Investigation for the Application of Second-Life Electric Vehicle Batteries for Behind-The-Meter Services, in: 2021 IEEE Electrical Power and Energy Conference (EPEC), IEEE, Toronto, ON, Canada, 2021, pp. 20–27, http://dx.doi.org/10.1109/EPEC52095.2021.9621638.

[71] I. Buratynskyi, T. Nechaieva, I. Leshchenko, S. Shulzhenko, Profitability of the PV Plant and BESS Joint Operation on the Electricity Market, in: A. Zaporozhets (Ed.), in: Systems, Decision and Control in Energy V, vol. 481, Springer Nature Switzerland, Cham, 2023, pp. 543–554, http://dx.doi.org/10.1007/978-3-031-35088-7_29, Series Title: Studies in Systems, Decision and Control.

[72] H. Shin, J. Hur, Optimal Energy Storage Sizing With Battery Augmentation for Renewable-Plus-Storage Power Plants, IEEE Access 8 (2020) 187730–187743, http://dx.doi.org/10.1109/ACCESS.2020.3031197.

[73] L. Tziovani, L. Hadjidemetriou, S. Timotheou, Optimizing the bidding strategy and assessing profitability of over-install renewable plants equipped with battery energy storage systems, Renew. Energy 234 (2024) 121247, http://dx.doi.org/10.1016/j.renene.2024.121247.

[74] E. Hossain, D. Murtaugh, J. Mody, H.M.R. Faruque, M.S. Haque Sunny, N. Mohammad, A Comprehensive Review on Second-Life Batteries: Current State, Manufacturing Considerations, Applications, Impacts, Barriers & Potential Solutions, Business Strategies, and Policies, IEEE Access 7 (2019) 73215–73252, http://dx.doi.org/10.1109/ACCESS.2019.2917859.

[75] Element Energy Announces Commissioning of World's Largest Second-Life Battery Storage Project, Tech. rep., 2024.

[76] Redwood Energy: fast, Low-Cost Storage to Power the Age of AI and a Changing Grid, Tech. rep., Redwood Materials, 2025.

[77] A.A. Adepoju, Q.L. Williams, High C-rate performance of LiFePO4/carbon nanofibers composite cathode for Li-ion batteries, Curr. Appl. Phys. 20 (1) (2020) 1–4, http://dx.doi.org/10.1016/j.cap.2019.09.014.

[78] F. Conte, S. Massucco, G.-P. Schiapparelli, F. Silvestro, Day-Ahead and Intra-Day Planning of Integrated BESS-PV Systems Providing Frequency Regulation, IEEE Trans. Sustain. Energy 11 (3) (2020) 1797–1806, http://dx.doi.org/10.1109/TSTE.2019.2941369.

[79] C. White, B. Thompson, L.G. Swan, Comparative performance study of electric vehicle batteries repurposed for electricity grid energy arbitrage, Appl. Energy 288 (2021) 116637, http://dx.doi.org/10.1016/j.apenergy.2021.116637.

[80] L. Di Persio, A. Cecchin, F. Cordoni, Novel approaches to the energy load unbalance forecasting in the Italian electricity market, J. Math. Ind. 7 (1) (2017) 5, http://dx.doi.org/10.1186/s13362-017-0035-y.

[81] M. Dubarry, A. Devie, K. Stein, M. Tun, M. Matsuura, R. Rocheleau, Battery Energy Storage System battery durability and reliability under electric utility grid operations: Analysis of 3 years of real usage, J. Power Sources 338 (2017) 65–73, http://dx.doi.org/10.1016/j.jpowsour.2016.11.034.

[82] N. Noyanbayev, A. Forsyth, T. Feehally, Efficiency analysis for a grid-connected battery energy storage system, Mater. Today: Proc. 5 (11) (2018) 22811–22818, http://dx.doi.org/10.1016/j.matpr.2018.07.095.

[83] A. Bonfitto, E. Ezemobi, N. Amati, S. Feraco, A. Tonoli, S. Hegde, State of Health Estimation of Lithium Batteries for Automotive Applications with Artificial Neural Networks, in: 2019 AEIT International Conference of Electrical and Electronic Technologies for Automotive (AEIT AUTOMOTIVE), IEEE, Torino, Italy, 2019, pp. 1–5, http://dx.doi.org/10.23919/EETA.2019.8804567.

[84] K.S. Ng, C.-S. Moo, Y.-P. Chen, Y.-C. Hsieh, Enhanced coulomb counting method for estimating state-of-charge and state-of-health of lithium-ion batteries, Appl. Energy 86 (9) (2009) 1506–1511, http://dx.doi.org/10.1016/j.apenergy.2008.11.021.

[85] GME, Dati di sintesi MPE-MGP – evoluzione giornaliera, Tech. rep., Gestore Mercati Energetici, 2024, URL https://www.mercatoelettrico.org/it/Statistiche/ME/GraphGiornaliero.aspx.

[86] Regulation (EU) 2024/1781 of the European Parliament and of the Council of 13 June 2024 establishing a framework for the setting of ecodesign requirements for sustainable products, amending Directive (EU) 2020/1828 and Regulation (EU) 2023/1542 and repealing Directive 2009/125/EC (Text with EEA relevance). URL http://data.europa.eu/eli/reg/2024/1781/oj/eng. Legislative Body: COM, GROW.

[87] T. Montes, M. Etxandi-Santolaya, J. Eichman, V.J. Ferreira, L. Trilla, C. Corchero, Procedure for Assessing the Suitability of Battery Second Life Applications after EV First Life, Batteries 8 (9) (2022) 122, http://dx.doi.org/10.3390/batteries8090122.

[88] N. Mukherjee, D. Strickland, Control of Second-Life Hybrid Battery Energy Storage System Based on Modular Boost-Multilevel Buck Converter, IEEE Trans. Ind. Electron. 62 (2) (2015) 1034–1046, http://dx.doi.org/10.1109/TIE.2014.2341598.

[89] C. Liu, X. Cai, Q. Chen, Self-Adaptation Control of Second-Life Battery Energy Storage System Based on Cascaded H-Bridge Converter, IEEE J. Emerg. Sel. Top. Power Electron. 8 (2) (2020) 1428–1441, http://dx.doi.org/10.1109/JESTPE.2018.2886965.

[90] X. Gu, H. Bai, X. Cui, J. Zhu, W. Zhuang, Z. Li, X. Hu, Z. Song, Challenges and opportunities for second-life batteries: Key technologies and economy, Renew. Sustain. Energy Rev. 192 (2024) 114191, http://dx.doi.org/10.1016/j.rser.2023.114191.

[91] H. Wang, M. Rasheed, R. Hassan, M. Kamel, S. Tong, R. Zane, Life-Extended Active Battery Control for Energy Storage Using Electric Vehicle Retired Batteries, IEEE Trans. Power Electron. 38 (6) (2023) 6801–6805, http://dx.doi.org/10.1109/TPEL.2023.3252362.

[92] M.T. Lawder, B. Suthar, P.W.C. Northrop, S. De, C.M. Hoff, O. Leitermann, M.L. Crow, S. Santhanagopalan, V.R. Subramanian, Battery Energy Storage System (BESS) and Battery Management System (BMS) for Grid-Scale Applications, Proc. IEEE 102 (6) (2014) 1014–1030, http://dx.doi.org/10.1109/JPROC.2014.2317451.

[93] J.A. Jeevarajan, T. Joshi, M. Parhizi, T. Rauhala, D. Juarez-Robles, Battery Hazards for Large Energy Storage Systems, ACS Energy Lett. 7 (8) (2022) 2725–2733, http://dx.doi.org/10.1021/acsenergylett.2c01400.

[94] J. Conzen, S. Lakshmipathy, A. Kapahi, S. Kraft, M. DiDomizio, Lithium ion battery energy storage systems (BESS) hazards, J. Loss Prev. Process. Ind. 81 (2023) 104932, http://dx.doi.org/10.1016/j.jlp.2022.104932.

[95] D. Ansean, M. Gonzalez, J.C. Viera, V.M. Garcia, J.C. Alvarez, C. Blanco, Electric Vehicle Li-Ion Battery Evaluation Based on Internal Resistance Analysis, in: 2014 IEEE Vehicle Power and Propulsion Conference (VPPC), IEEE, Coimbra, Portugal, 2014, pp. 1–6, http://dx.doi.org/10.1109/VPPC.2014.7007058.

[96] Y. Sun, F. Liu, W. Qin, J. Li, X. Cheng, J. Zeng, Dynamic internal resistance modeling and thermal characteristics of lithium-ion batteries for electric vehicles by considering state of health, J. Power Sources 612 (2024) 234806, http://dx.doi.org/10.1016/j.jpowsour.2024.234806.

[97] V.J. Ovejas, A. Cuadras, Effects of cycling on lithium-ion battery hysteresis and overvoltage, Sci. Rep. 9 (1) (2019) 14875, http://dx.doi.org/10.1038/s41598-019-51474-5.

[98] J. Duan, X. Tang, H. Dai, Y. Yang, W. Wu, X. Wei, Y. Huang, Building Safe Lithium-Ion Batteries for Electric Vehicles: A Review, Electrochem. Energy Rev. 3 (1) (2020) 1–42, http://dx.doi.org/10.1007/s41918-019-00060-4.